Interaction of Acetic Acid with Solid Water

S. Bahr,[†] A. Borodin,[†,§] O. Höfft,[†] V. Kempter,*[,†] A. Allouche,[‡] F. Borget,[‡] and T. Chiavassa[‡]

Institut für Physik und Physikalische Technologien, Technische Universität Clausthal, D-38678 Clausthal-Zellerfeld, Germany, Physique des Interactions Ioniques et Moléculaires, Université de Provence and CNRS, Unité Mixte de Recherche N°6633, Campus de Saint Jérôme Service 242, 13397 Marseille Cedex 20, France, and Department of Chemistry, Graduate School of Science, Tohoku University, Aoba-ku, Sendai 980-8578, Japan

Received: October 19, 2005; In Final Form: March 9, 2006

The interaction of acetic acid (AA, CH_3COOH), with solid water, deposited on metals, tungsten and gold, at 80 K, was investigated. We have prepared acid/water interfaces at 80 K, namely, acid layers on thin films of solid water and H_2O adlayers on thin acid films; they were annealed between 80 and 200 K. Metastable impact electron spectroscopy (MIES) and ultraviolet photoelectron spectroscopy UPS(HeII) were utilized to obtain information on the electronic structure of the outermost surface from the study of the electron emission from the weakest bound MOs of the acids, and of the molecular water. Temperature-programmed desorption (TPD) provided information on the desorption kinetics, and Fourier-transformed infrared spectroscopy (FTIR) provided information on the identification of the adsorbed species as well as on the water and acid crystallization. The results are compatible with the finding of ref 1 (preceding paper), made on the basis of DFT calculations, that AA adsorbs on ice as cyclic dimers. Above 120 K, a rearrangement of the AA dimers is suggested by a sharpening of the spectral features in the IR spectra and by spectral changes in MIES and UPS; this is attributed to the glass transition in AA around 130 K. Above 150 K the spectra transform into those characteristic for polycrystalline polymer chains. This structure is stable up to about 180 K; desorption of water takes place from underneath the AA film, and practically all water has desorbed through the AA film before AA desorption starts. There is no indication of water-induced deprotonation of the acid molecules. For the interaction of H_2O molecules adsorbed on amorphous AA films, the comparison of MIES with the DFT results of ref 1 shows that the initial phase of exposure does not lead to the formation of a top-adsorbed closed water film at 80 K. Rather, the H_2O molecules become attached to or incorporated into the preexisting AA network by H bonding; no water network is formed in the initial stage of the water adsorption. Also under these conditions no deprotonation of the acid can be detected.

1. Introduction

The interaction of acids with ice surfaces is not well understood at present. Even for the well-studied HCl/water ice system, the conditions under which ice promotes the dissociation of acids are still under debate.[2−5] For the carboxylic acids formic and acetic acid (FA and AA, respectively) interacting with ice surfaces, free energy profiles obtained from classical MD calculations demonstrate that carboxylic acids are strongly trapped at the ice surface at 250 K.[6] Caused by the ability to form strong H bonds with the ice surface and among themselves, the adsorption process can be quite complicated: on one hand, it is predicted that the interaction of isolated AA species with ice leads to the dissociation of AA dimers,[7] but, on the other hand, the interaction between adsorbed monomer species near monolayer coverage of the ice surface may lead to the reformation of AA oligomers.[7] On the basis of TOF-SIMS measurements for AA, initially top-deposited on water ice, it was concluded that solvation is incomplete, and at least the methyl group is not completely covered by water molecules.[8] However, the corresponding results for FA on ice suggested that the adsorbates become hydrated above 110 K and a water toplayer is formed at 140 K, that is, full solvation takes place.[9] Combined EELS and TPD results, obtained during the coadsorption of FA and H_2O on Pt surfaces in the range from 100 to 200 K suggested that incomplete solvation takes place, that is, FA−H_2O complexes (1:2...3 stoichiometry) are formed. A model was favored in which small water aggregates become attached to FA chains.[10] Still more recently, the change of the morphology of AA films was studied by TPD (temperature-programmed desorption spectroscopy).[11] With the analytical techniques at our disposal, MIES (metastable impact electron spectroscopy),[12,13] UPS, and TPD, we have studied the FA−water interaction[14] and have compared the results with DFT cluster calculations.[15]

To gain a more detailed understanding of the interaction between water and carboxylic acids, we have included the interaction of AA with water into our studies, and, moreover, have added IR spectroscopy to the scope of our techniques MIES, UPS, and TPD. IR spectroscopy is applied to identify the adsorbed species, to obtain detailed information on the lateral interaction among the AA species themselves and with H_2O, and to determine the role that an eventual amorphous (or liquid)-to-crystalline phase transition may play for the acid−water interaction. We follow the same strategy as that in refs 14 and 15 and compare our electron spectroscopy results with the

* Corresponding author. Tel: ++49-5323-72-2363. Fax: ++49-5323-72-3600. E-mail: Volker.Kempter@tu-clausthal.de.
[†] Technische Universität Clausthal.
[‡] Université de Provence.
[§] Tohoku University.

10.1021/jp055980u CCC: $33.50
Published on Web 04/08/2006

density of states (DOS) and the desorption energies supplied by DFT calculations carried out on the AA−water system (preceding paper[1]). The interpretation of our results is facilitated by the recent IRAS work on the AA−ice interaction[16] and DFT calculations for the hydration of AA monomers.[17]

2. Experimental Details

2.1. Electron Spectroscopy. Experimental details on the apparatus employed for the electron spectroscopic studies can be found in refs 14 and 18 where the ice surface[18] and the FA/ice interaction[14] were studied. Briefly, the UHV apparatus is equipped with a cold-cathode gas discharge source for the production of metastable atoms (about 20 eV potential energy) of thermal kinetic energy for metastable impact electron spectroscopy (MIES) and HeI photons ($E^* = 21.2$ eV) as a source for ultraviolet photoelectron spectroscopy (UPS). Because the metastable atoms approach the surface with near-thermal kinetic energy (60−100 meV), MIES is nondestructive and highly surface-sensitive (see refs 12 and 13 for more detailed introductions into MIES and its various applications in molecular and surface spectroscopy). A second photon source is at our disposal providing HeI and HeII (40.8 eV) photons. When starting the sources the base pressure of the chamber rises from 2×10^{-10} Torr to 5×10^{-9} Torr (He) and stays nearly constant during the measurements. The sample can be cooled with LN_2 to 80 K. The surface was exposed to AA or water by backfilling the chamber. The exposures are stated in Langmuirs (L) (1 L $= 10^{-6}$ Torr·s). The amount of surface-adsorbed water can be estimated on the basis of our previous results concerned with the water−titania interaction,[18] and 4 L correspond to about 1 bilayer of water. Because the water signals have disappeared after about 4 L of AA were offered, we conclude, on the basis of the ultrasurface sensitivity of MIES, that at this stage AA monolayer coverage has been reached.

Annealing of the prepared films is done stepwise; during the collection of the MIES or UPS spectra, we keep the substrate temperature constant.

2.2. Temperature-Programmed Desorption (TPD). The TPD experiments are carried out using a differentially pumped quadrupole mass spectrometer (Balzers QMG 422), connected to the UHV apparatus employed for the MIES/UPS studies. To obtain TPD spectra exclusively from the relevant surface area, we surround the QMS with a stainless steel housing with an 3 mm opening. This opening is positioned approximately 1 mm in front of the sample during the measurements. The TPD spectra are collected at a linear heating rate of 1 K/s, and routinely five different masses are measured simultaneously. Under these circumstances, we see the onset of desorption in the MIES/UPS spectra (data collection time 60 s per spectrum) about 15 K below the desorption peak maximum temperature. The acid/water and water/acid films for TPD measurements are prepared as described in Section 2.1.

2.3. Infrared Spectroscopy. The experimental technique used here has been described in the literature.[19,20] Briefly, the apparatus consists of a turbo-pumped sample chamber containing a gold-plated mirror, directly mounted to a cryostat, cooled by an He compressor unit, held at low temperature (80−210 K). The sample is surrounded by a gold-plated shield held at approximately 80 K, irrespective of the actual sample temperature, guaranteeing a low rate for impurity deposition and water-free vacuum. So the amount of water deposited from the residual gas during the AA film deposition as well as during the film annealing is negligible. The chamber is coupled to a Fourier-transform infrared spectrometer (Nicolet Magna 750) equipped with a liquid-N_2-cooled mercury-cadmium-telluride (MCT)-detector (energy range 600−7000 cm^{-1}), a Ge-coated KBr beam splitter, and a globar source. The IR spectra are recorded in reflection mode: the photon beam is reflected from the gold mirror under under 4° to the surface normal, thereby passing twice the films frozen onto it. H_2O and AA were degassed successively by several freeze−pump−thaw cycles before each use. Amorphous ice films were obtained from a water/argon (1:50) gaseous mixture deposited at 80 K with a 1 nm/s growth rate. The deposition was made under a constant pumping in order to outgas Ar. In addition, the use of a carrier gas allows good control of the ice deposition. If not mentioned otherwise, the film thicknesses utilized for the IR studies are about 0.1 μm as can be deduced from calibration of the infrared absorbance changes versus film thickness using optical interference.[19] Similarly, acid molecules, diluted by Ar (1:2000), were deposited at 80 K on Au and on water films. After acid deposition, the sample was heated from 80 K up to 210 K, a temperature leading to complete sublimation of both acid and water.

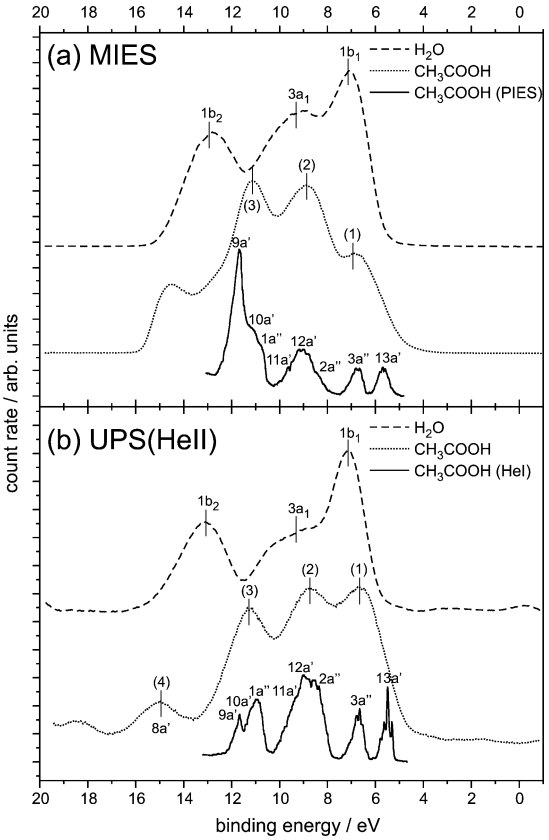

Figure 1. MIES (a) spectra of acetic acid (AA) (42 L) and water (18 L) films and UPS(HeII) (b) spectra (AA (23 L); H_2O (24 L)) prepared at 90 K. Also shown are the Penning ionization (PIES) and UPS(HeI) spectra from gaseous, free AA molecules.

The spectra reported herein have been recorded in the 650−4000 cm^{-1} wavenumber range with a 1 cm^{-1} resolution, between 80 and 200 K. As the temperature was ramped with a constant heating rate of 1 K/min, 100 interferograms were accumulated every 5−10 K interval. The collection of one complete IR spectrum required approximately 1 min.

3. Results

3.1. Electron Spectroscopy. *3.1.1. Signature of Acetic Acid Species in MIES and UPS.* Figure 1 compares the present MIES and UPS(HeII) spectra of AA multilayers with Penning ionization electron spectra (PIES) and UPS(HeI) spectra of isolated

AA monomers.[21] Similar differences are seen between the spectra of monomers and condensed species as in ref 14 for FA: it was noticed that the FA-induced spectra are characteristically different from the UPS(HeI) and PIES spectra of isolated FA monomers[21−23] and must be attributed to FA species displaying strong lateral interactions among each other. The HeI spectra reported for AA dimers in the gas phase[22,23] show essentially a three-peaked structure similar to, although not identical to, the present MIES and UPS spectra for condensed AA. Peak 4 seen with HeII is not found in MIES because the potential energy of He* is insufficient to eject electrons with binding energies larger than about 15 eV. As for FA, we conclude that contributions to structures 1 to 4 are due to the ionization of the MOs 3a″; 13a′ (1), 2a″; 12a′ (2), 1a″; 10a′; 9a′ (3), and 8a′ (4) mainly.

The deviations seen in the spectra for condensed AA, with respect to the available gas-phase spectra, are independent of the type of substrate employed for condensation; that is, the same spectra are seen for the adsorption on tungsten, gold, and water as for the multilayered acid species. This suggests that the lateral interaction between acid molecules is important and that the spectra show features typical for condensation, even at the lowest exposures. Peak 1, caused mainly by the carbonyl (C═O) group, is relatively weak in the MIES spectra (as compared to 2 and 3) while it dominates in the HeII spectra. We attribute this behavior to the fact that the carbonyl group mediates the bond within the multilayers and is not easily accessible to the interaction with the He* atom and is seen with reduced intensity.

3.1.2. Interaction of Acetic Acid with Water Films and Vice Versa. The general structure of the MIES and UPS(HeII) spectra, recorded during the interaction of water multilayers with AA and vice versa is, in the entire studied range of temperatures, rather similar to those displayed in Figure 1 and, therefore, is not reproduced here (for details see ref 24). As compared to HeII, the intensity of feature 1 appears to be reduced in MIES, providing evidence for prediction of theory that the carbonyl group is directed toward the water film.[6,7,15]

Figure 2 presents the temperature dependence of particular spectral features ($1b_1$ H_2O and peak 2 of AA) in the MIES and UPS(HeII) spectra for AA on water films (a) and vice versa (b); the spectra required for the peak analysis are taken from ref 24. A closed AA adlayer is present on the multilayered water after preparation (exposure 4 L AA). Alternatively, an exposure of 7 L H_2O is not sufficient to produce a closed water adlayer on AA films: the spectra display both H_2O and AA features prior to heating. The same behavior was noticed for the interaction of FA and water.[14] We have examined the exposure dependence of the H_2O and AA signals in MIES and UPS(HeII) during film preparation. From that comparison, we conclude that clustering of H_2O on AA is not responsible for the fact that water does not block the AA surface from the access of the He* atoms. TOF-SIMS results for a monolayer of AA, deposited on multilayers of amorphous solid water, suggest that the CH_3 group of AA is not fully covered by D_2O, and, thus, AA is at most partially solvated up to water desorption.[8] It was supposed that a mixed structure is formed, whereby H_2O molecules may become attached to or incorporated into the AA network similar to what was discussed in refs 25−27. Consistent with these findings, our MIES results clearly show that the toplayer of the system contains AA species at all temperatures, up to water desorption.

The strong decrease of the water signal observed around 148 K for AA/H_2O and around 138 K for H_2O/AA is due to water desorption. Correlated with this decrease is a partial decay of the AA signal that we attribute to AA desorption; codesorption of H_2O and AA has already been noticed in ref 16. However, in contrast to water, AA does not fully desorb before 185 K. More details on the desorption process are obtained from TPD (see Section 3.2).

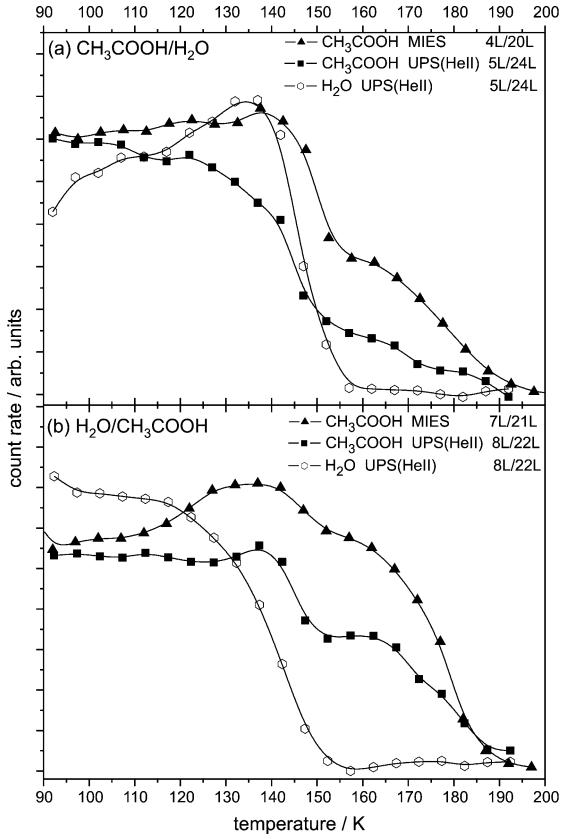

Figure 2. Temperature dependence (90−200 K) of selected spectral features ($1b_1$ H_2O and peak 2 of AA) in the MIES and UPS(HeII)-spectra (multiplication factor 3.8 for AA and 3.2 for H_2O) for AA on water (5−6 BL) (a), and for water (2 BL) on AA films (b). The spectra required for the peak analysis are taken from ref 24.

3.2. TPD Spectra. The TPD spectra for the AA−water system in the range from 120 to 250 K, are presented in Figure 3 for AA on ice films (a) and H_2O on films of solid AA (b). They are rather similar, irrespective of the order of adsorption. Caused by the considerably longer time required to complete data collection in MIES (1 min as compared to 1 s for TPD), desorption is complete in MIES about 15 K before the desorption peak maxima are reached in TPD.[14] The same behavior has been noticed for the corresponding changes observed in HREELS and TPD spectra from H_2O and FA codeposition on Pt(111).[10]

No shoulder due to water crystallization is observed around 150 K,[28] probably because of the relatively fast heating rate and due to the AA−H_2O interaction. We observe simultaneous desorption of H_2O and AA between 140 and 165 K[16] (see the shoulder in the AA signal located around 157 K). But, although water has essentially desorbed below 170 K (desorption peak maximum around 160 K), a relatively small amount of AA has desorbed up to this temperature. This implies that the desorption of a water layer, originally prepared underneath a AA toplayer, desorbs through the AA toplayer. As auxiliary studies with AA on tungsten show, most of the AA desorbs above 170 K, in the range where AA multilayers are found to desorb (desorption peak around 180 K). The high-temperature tail, above 190 K, is due to AA species chemisorbed on the tungsten substrate.

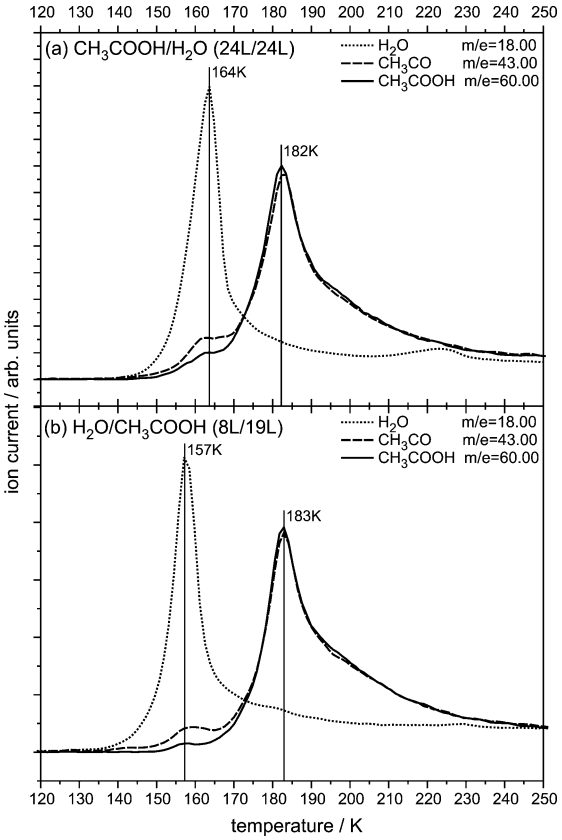

Figure 3. Thermal desorption (TPD) traces for AA on water (5.5 BL) (a) and for H_2O (4 BL) on AA (b) between 120 and 250 K. Mass 18: water; mass 43 and 60: acetic acid (multiplication factors 1, 20, and 60 in a and 1, 10, and 30 in b, respectively).

3.3. Infrared Spectroscopy. The IR spectrum of ice (Figure 4) displays the OH bulk stretching modes of ice, broad and intense, around 3250 cm^{-1}, then the OH bending modes, around 1640 cm^{-1}, and a broad feature at 840 cm^{-1}, assigned to the libration modes of water molecules in the bulk. In addition, we observe the dangling OH mode at 3695 cm^{-1} (3696 cm^{-1} in ref 16) where the H atom is not involved in a hydrogen bonding. This dangling OH feature is a good probe for testing the adsorption of molecules on amorphous ice films.[29−31] A characteristic shift of the absorption from the OH stretching mode takes place around 150 K, accompanied by a sharpening of the respective structure. This is attributed to the crystallization of the initially amorphous ice film.[16,28,32] Water desorption takes place between 150 and 170 K.

Figure 5 displays the typical IR spectra of an AA film (0.1 μm thick) deposited on amorphous solid water (water part a, and AA part b). After the AA deposition at 80 K, the sample was heated to 190 K, a temperature leading to complete sublimation of both acid and water. Also displayed is the peak evolution as a function of annealing temperature in various spectral regions (c), in particular those with the OH bulk stretching modes of water and the νC−O and νC═O stretching modes of AA.

The assignment of the vibration bands is given in Table 1, and the positions of the spectral features agree with those reported in refs 16 and 33. The spectrum for AA on amorphous ice recorded at 80 K is very close to that of gas-phase AA dimers, as far as the main spectral features, in particular those of the (C−O) and (C═O) stretch vibrations, are concerned.[34,35] In particular, the spectra show two prominent features at 1705 and 1303 cm^{-1}, which can be attributed to the C═O and C−O stretching modes, respectively. Both of these features display

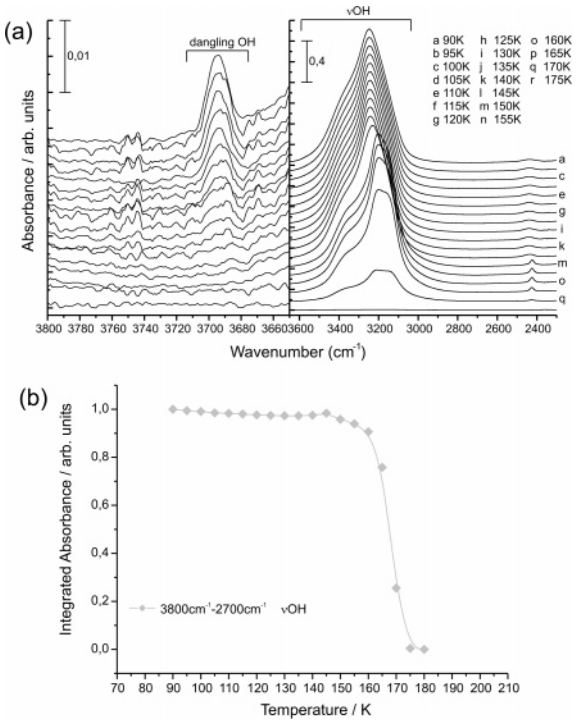

Figure 4. IR spectra of H_2O deposited on Au at 80 K, and spectra obtained during the annealing of the ice film from 80 to 180 K. Spectra between 3800 and 2300 cm^{-1} (a) and evolution of various peak areas during annealing (b).

shoulders toward lower wavenumbers, also seen for AA on Au, indicative for the presence of AA species whose (C═O) and (C−O) groups are more strongly distorted than in the cyclic dimers. A similar structure, seen in particular around 1294 and 1695 cm^{-1}, was attributed to AA species in direct contact with the ice surface.[16] Because we also see these structures for AA multilayers on Au, it appears plausible to attribute the two shoulders to the C═O and C−O stretch of dimers and small oligomers other than cyclic dimers that form during the film preparation.

As already noticed in ref 16, the spectra change drastically around 150 K and develop features characteristic for the crystalline phase. In the crystalline phase the AA species are known to exist as chainlike polymers.[25] Most notably, the strong features from the stretching modes mentioned above are replaced by the corresponding ones at 1646, 1660, and 1280 cm^{-1}, which, according to ref 36, are characteristic for (C═O) and (C−O) groups in AA polymer chains. The present assignment of the 1280 cm^{-1} absorption is at variance with ref 16 where it is attributed to νC−O of bulk monomers. The phase transition is characterized by the appearance of an additional (C−O) stretch feature, which signals the presence of an AA species whose (C−O) group is more strongly distorted than that in the cyclic dimer. Finally, desorption of AA takes place around 175 K while H_2O desorption is already noticeable around 155 K. In addition, a new broad feature appears between 1710 and 1760 cm^{-1}, which, according to ref 16, can be attributed to the (C═O) stretching mode of AA monomers, trapped in the bulk, but not directly interacting with the bulk structure. The phase transition also manifests itself in Figure 5c: the νC═O intensity increases sharply around 150 K; this can be explained by an increase of the dipole moment of the (C−O) group in its new chemical environment.[16] An indirect manifestation of the phase transition was also seen in TOF-SIMS as a sudden evolution of ions from the Ni substrate and was attributed to a structural relaxation.[11]

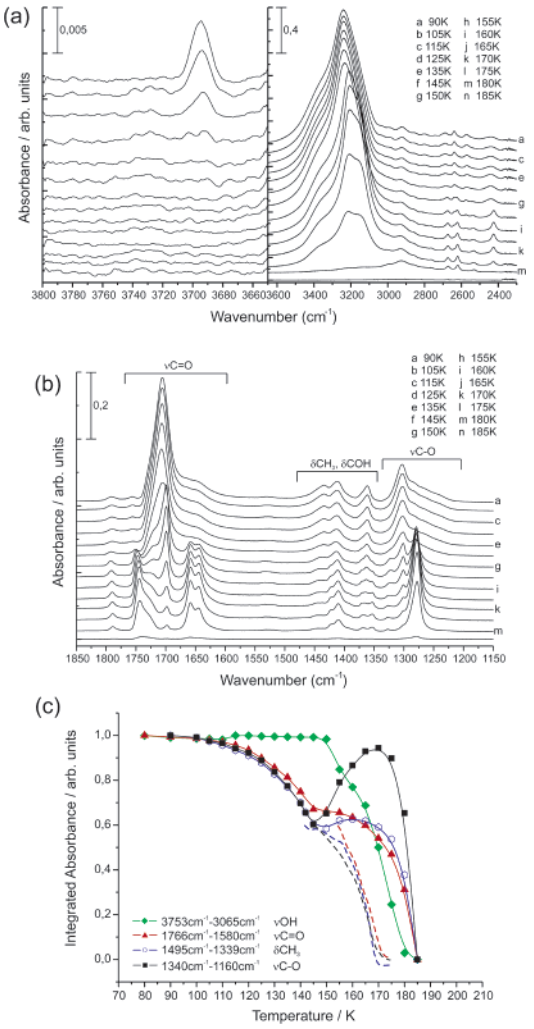

Figure 5. IR spectra for AA on ice, deposited on Au at 80 K, and spectra obtained during the annealing of the AA/ice film from 80 to 190 K. Spectra between 3800 and 2200 cm^{-1} (a), spectra between 1850 and 1150 cm^{-1} (b), and evolution of various peak areas during annealing (c).

When thin AA adlayers are deposited on ice films (reduction of the absorbance to 0.02), the crystallization (seen above 155 K for thicker films) does not take place. In particular, the nonmonotonic behavior of νC−O and νC═O is not observed, and the respective intensities decay as indicated by the dashed lines shown in Figure 5.

In the IR spectra, recorded from a water film deposited at 80 K on amorphous AA (see Figure 6), the spectral features from both H_2O and AA are found at the same positions and possess the same shapes as those seen in Figure 5 (see Figure 6a and Table 1). The crystallization of both AA and H_2O occurs around 150 K; as discussed above, the AA crystallization causes the rise of the νC−O signal (see Figure 6c). The desorption of H_2O and AA takes place at rather different temperatures, 155 and 180 K, respectively; that is, water molecules interacting with amorphous AA films desorb about 20 K earlier than when the water film is covered by an AA layer. As in the IR spectra for AA on the Au substrate (not shown), the dimer structures sharpen considerably around 130 K, accompanied with the disappearance of the shoulder associated with νC−O. This occurs in the temperature range where AA diffusion becomes important.[11] In contrast to AA on ice films, AA desorption is not noticeable before all water has desorbed. Spectra show no significant changes when the thickness of the water film is reduced by 1 order of magnitude (reduction of the absorbance to 0.02).

In addition, we have studied the H_2O interaction with polycrystalline AA films (not shown). According to IR, the water desorption takes place for $T > 170$ K, indicative for a stronger interaction of H_2O with the chains than with the cyclic dimers.

We have also studied the codeposition of water and AA (relative amount 1:2) on Au at 80 K, which leads to the cyclic dimer structure. Spectra versus temperature are quite similar to those for AA films on ice, in particular as far as the correlation between dimer-to-chain transition and water desorption is concerned. Judging from the larger height of the shoulders in the IR spectra relative to the intensity of the sharp νC−O and νC═O features, we conclude that, as a consequence of the water, the AA film is less ordered than when deposited on Au. This appears to be supported by the fact that the reordering of the film, observed at 130 K on Au, is also delayed until 160 K.

As a guide for the interpretation of the IR spectra for AA, we have also studied those of FA interacting with ice. They are in general agreement with the literature[37−40] (for details see ref 24).

4. Interpretation

In the following, a comparison will be made with the DFT results of ref 1. As in ref 14, it is assumed that, to a good approximation, the MIES spectra can be compared with that contribution to the DOS that comes from the uppermost layer of the AA−ice system. However, the UPS(HeII) spectra are closer to the computed total DOS.[14] IR spectra were also computed routinely during the work on ref 1; however, a comparison with the experiments is not presented here because quantitative agreement could not be obtained, and, furthermore, the identification of the spectral features seen in the IR spectra follows already from previous experimental work.

4.1. Electronic Structure of the Acid−Water System. It was proposed that, as for FA, the first adlayer consists of AA species that are strongly H bonded to the ice surface via their carbonyl groups,[6,16] and, at sufficiently large coverage, also display a strong lateral interaction.[6] However, the first-principles calculations of ref 1 predict that the cyclic dimer ($2AA_1$ in Figure 4 of ref 1)) represents the preferential mode of AA adsorption on ice, and consists of species whose molecular plane is parallel to the ice surface; they are bonded to the ice surface via two H bonds, involving the C═O and O−H groups of the AA species. The IR results on AA films identify two forms of condensed AA, cyclic AA dimers below about 150 K and AA chains after crystallization. This lends support to the prediction of ref 1 and is taken as justification to compare the MIES and UPS(HeII) results with the DOS of the interface between AA cyclic dimers and ice.

Figure 7a compares the contribution of the DOS resulting solely from the AA dimer (projection i) with the MIES spectrum for about 0.6 ML AA deposited on ice (considering the fact that MIES is sensitive to the toplayer only). Also shown is the total DOS of the $2AA_1$ configuration. Figure 7b compares the corresponding UPS(HeII) spectra with the contribution to the DOS resulting from both the AA dimer and the uppermost water bilayer (projection ii), thereby taking into account the larger depth information of HeII. As in the experiment, the largest difference is in the magnitude of peak 1 (due to the large contribution of $1b_1$ H_2O to the "surface-near" DOS of Figure 7b). Both the MIES and HeII spectra are predicted quite well; however, structure 1 in the surface DOS resembles a shoulder rather than a peak as in the experiment.

The agreement between theory and experiment can be improved, in particular as far as peak 1 is concerned, by taking

TABLE 1: Identification of the Spectral Features Seen in the IR Spectra of Figures 4, 5, and 6; All Values Are in cm^{-1}

solid CH_3COOH 80 K	solid CH_3COOH 150 K	CH_3COOH on amorphous ice film 80 K	CH_3COOH on crystalline ice film 155 K	assignments[a]
3085	3085			$\nu C{=}O + \delta COH$
3024		3024		νOH
2982	2995	2995		$\nu_{as}CH_3$
2920	2940	2940	2928	$\nu_s CH_3$
2855	2864	2864	2862	$2\delta COH$
2799	2764	2764	2815/2764	$2\delta_{as}CH_3$
2739	2712	2712	2714	$2\delta_s CH_3$
2687	2672	2672	2674	$\nu C{-}O + \delta COH$
2638	2619	2619	2635/2622	$\nu C{-}O + \delta_s CH_3$
2572	2531	2531	2574/2535	$2\nu C{-}O$
1790	1787	1787	1791	$\nu C{=}O$ (M_S)
1755			1747	$\nu C{=}O$ (M_B)
	1723	1723	1720	$\nu C{=}O$ (D)
1699	1697*	1705	1699	$\nu C{=}O$ (D)
1666*	1659		1660	$\nu C{=}O$
1643*	1648	1651	1646	$\nu C{=}O$
	1533	1533	1534	$\delta OCO + \nu C{-}O$
1431	1447/1436	1432	1440	δCOH
1410	1408	1412	1412	$\delta_{as}CH_3$
1360	1363/1351	1361	1363	$\delta_s CH_3$
	1326		1322	$\nu C{-}O$ (D)
1300		1303	1301	$\nu C{-}O$
1281*	1273	1283	1280	$\nu C{-}O$

[a] ν, stretching; δ, bending in plane; M_S, AA monomers located on the surface; M_B, AA monomers trapped into the bulk; D, peak according to dimerized AA; *, contained in amorphous or crystalline AA in a weak amount.

the hydration of the cyclic AA dimers into account. It was predicted that the H_2O−AA dimer interaction leads to the breakup of those dimers that come into direct contact with the adsorbed H_2O, and that, as a consequence, mixed rings are formed by the incorporation of the H_2O into the cyclic dimer structure.[26] In fact, the results in ref 1 show that the mixed ring, consisting of 2AA and $1H_2O$ molecules ($2AAH_1$, in Figure 6 of ref 1) is rather stable. However, the absence of water-induced changes in the 120−150 K temperature range (where hydration phenomena can be expected to become important) in any of the spectra lets us discard $2AAH_1$ as the actual hydrated AA structure. Instead, we assume for the comparison with the MIES and HeII results that the hydration consists of the attachment of one H_2O molecule to the AA dimer in the way shown in Figure 8 (inset) (denoted by $2AAH_2$ in ref 1). Figure 8a compares the contribution of the DOS resulting solely from the AA dimer and the H_2O molecule outside the uppermost bilayer (projection i) with the MIES spectrum for about 0.5 ML AA deposited on ice. Also shown is the total DOS of the $2AAH_2$ configuration (see Figure 6 and Table 3 of ref 1). Figure 8b compares the corresponding UPS(HeII) spectra with the contribution to the DOS resulting from both the hydrated AA dimer and the uppermost water bilayer (projection ii). The increase of peak 1 in the DOS is due to the contribution of the $1b_1$ MO of water to the DOS shoulder from the 3a″ and 13a′ MOs of AA. This brings the resulting partial DOS in better agreement with the MIES spectrum. A shoulder can be noticed around 13 eV, which is due to the water $1b_2$ MO.

A detailed comparison of the spectra obtained for the adsorption of H_2O on condensed AA with the results of ref 1 for the interaction of H_2O with a crystalline AA surface will not be presented here: we have compared the MIES spectra with the structure $(101)_A$ of ref 1, which predicts the strongest interaction of H_2O molecules with a crystalline AA surface. However, the DOS, appropriate for the comparison with MIES, gives too small of a contribution to peak 1. A closer inspection reveals that the particular orientation of the AA molecules in $(101)_A$ gives too small of a surface DOS contribution to peak 1. This disagreement is not too surprising because the AA film studied with MIES is amorphous, rather than crystalline.

A qualitative description of the H_2O interaction with condensed cyclic AA dimers is provided by the attachment of individual (up to two) water molecules to the dimers by H bonds. This can be demonstrated qualitatively in the following manner: we have extracted from the configuration $2AAH_2$ (see ref 1 and the inset in Figure 8) the partial DOS of the complex consisting of the dimer and the two H_2O's that form H bonds with the AA dimer. The partial DOS (not reproduced) is essentially as shown in Figure 8, but with a slight enhancement of peak 1, and is in reasonable agreement with the MIES spectrum for 2 L H_2O adsorbed on condensed AA. This model can also explain the experimental finding that a large exposure of water is required to form a closed water overlayer atop of the AA film: the two water molecules that can be attached to an individual cyclic AA dimer via H bonds are unable to shield the AA dimer from the access of the He* probe atom.

4.2. Adsorption and Desorption Processes in the AA−Water System. An understanding of the temperature dependence of the spectral intensities (Figures 2−6) can be achieved on the basis of the desorption energies reported in ref 1. We first consider the AA−ice interface: strong interaction exists between the AA species in the cyclic dimer (dimerization energy 79.3 kJ mol^{-1}), while the mutual interaction between two hydrated dimers on ice is small, of the van der Waals type only. However, the vertical interaction between the hydrated dimer and the ice surface (57 kJ mol^{-1} for $2AAH_2$) is comparatively strong and of the same magnitude as that between H_2O and ice (64.7 kJ mol^{-1}). This suggests that AA dimers desorb together with H_2O molecules and that the correlation seen in the TPD and MIES/UPS(HeII) intensities for H_2O and AA between 140 and 160 K is due to the simultaneous desorption of both species. Alternatively, the decrease of intensity seen with IR between 110 and 145 K is not seen with MIES/UPS(HeII), TPD, or TOF-SIMS. Thus, it cannot be attributed to desorption of AA and is probably due to a decrease of the dipole moment of the IR-

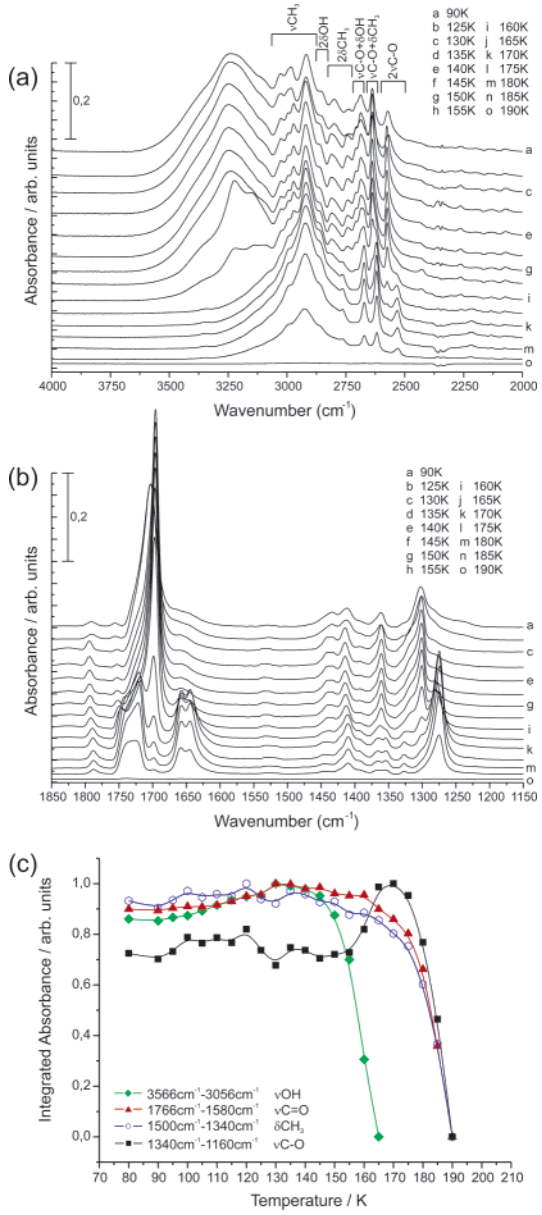

Figure 6. IR spectra for H_2O on an AA film, deposited on Au at 80 K, and spectra obtained during the annealing of the H_2O/AA film from 80 to 190 K. Spectra between 3800 and 2200 cm^{-1} (a), spectra between 1850 and 1150 cm^{-1} (b), and evolution of various peak areas during annealing (c).

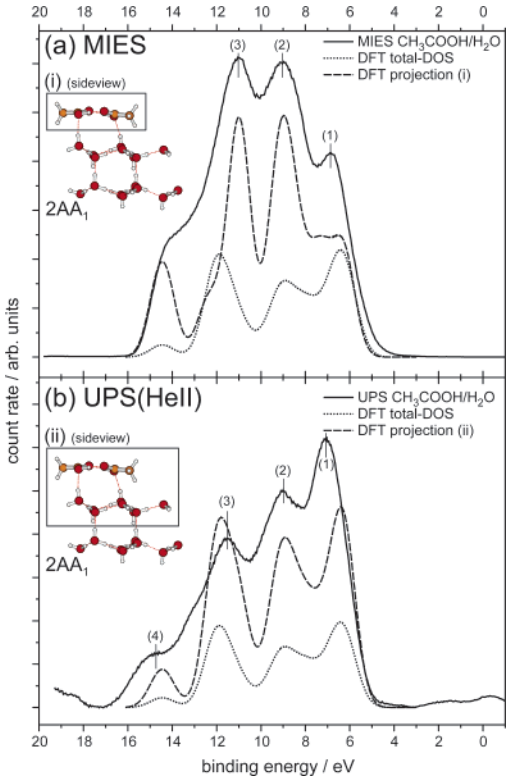

Figure 7. DOS for cyclic acetic acid dimers on top of a water film in comparison with experimental MIES (a) and UPS(HeII) (b) data for 1.5 L AA (a) and 5.2 L AA (b) deposited at 80 K on a water film (5 BL). Dotted line: total DOS. Dashed line: contribution from the dimer only (projection i) and from both the dimer and the uppermost water bilayer (projection ii). DFT projection is magnified by a factor of eight.

active groups, in particular C−O and C═O, caused by the onset of their hydration.

The early desorption of H_2O from AA films (as compared to H_2O desorption from ice) noticed with MIES/UPS and IR implies that the H_2O interaction with condensed AA is weaker than that with ice. We suggest that the specific structure of the AA network, in particular the presence of the hydrophobic methyl groups, inhibits the formation of a water network with strong lateral interactions. Under these circumstances the interaction of single H_2O molecules with crystalline AA, being less than 46.1 kJ mol^{-1} (as compared to 64.7 kJ mol^{-1} from ice), is relevant for H_2O desorption.

As clearly noticeable from the temperature dependence of the νC−O and νC═O intensities in Figure 5c, the AA film consisting of cyclic dimers transforms into the chain structure, typical for the polycrystalline AA bulk,[16,36] and remains stable up to more than 180 K. This rather high desorption temperature signals a strong lateral interaction between the AA species in the chains. As a consequence of the strong lateral interaction in crystalline AA, water desorption takes place through the polycrystalline AA film above about 150 K. Judging from the high temperature for desorption of AA multilayers (>180 K), the lateral interaction energy between AA species must be larger than the dimerization energy of the cyclic dimer of 79 kJ mol^{-1} (ref 1), suggesting that two strong H bonds are responsible for the bonding of AA species in the chain structure. It is suggested in ref 1 that a concerted proton transfer involving two cyclic dimers, stacked on top of each other, leads to the reorganization of the H bonds required for the chain formation. As a consequence, this transformation becomes feasible at little cost of energy.

Finally, we comment on the sharpening of, in particular, the νC═O and νC−O structures in IR seen around 130 K: there, for AA/gold and H_2O/AA the shoulders associated with the νC═O and νC−O structures of the dimers largely disappear, without a noticeable loss of total intensity. Hereby, the spectral features associated with the dimer structure simply sharpen considerably, without a concomitant qualitative change of the spectra being noticeable. The observed spectral changes may be related to an amorphous solid-to-supercooled liquid transition occurring in AA, initiated by the onset of the translational molecular diffusion (glass transition);[28] in water and ethanol such a transition occurs around 136 K and 97 K, respectively (see ref 41 and references given therein). Provided that this interpretation is correct, the glass transition temperature in AA would be around 130 K; that is, close to the value of water. We point out that a solid-to-liquid transition is not obvious for AA/ice.

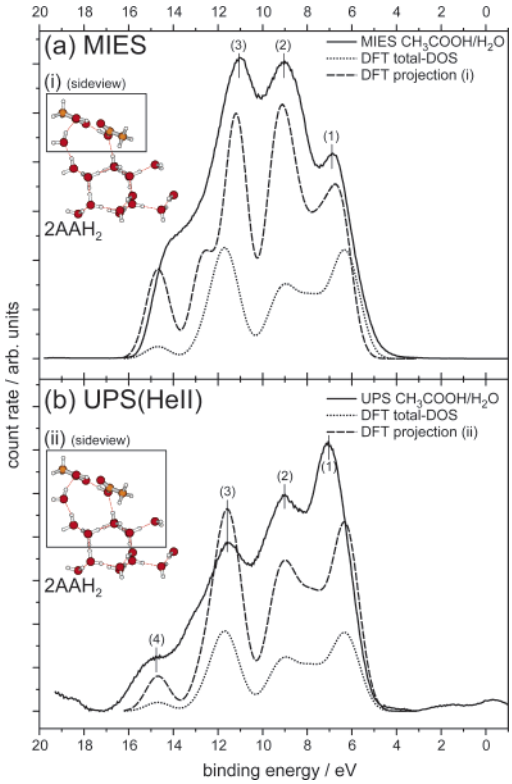

Figure 8. DOS for hydrated cyclic acetic acid dimers on top of a water film in comparison with the experimental MIES (a) and UPS(HeII) (b) data for 1.5 L AA (a) and 5.2 L AA (b) deposited at 80 K on a water film (5 BL). Dotted line: total DOS. Dashed line: contribution from the dimer and the H_2O outside the water bilayer (projection i) and including the contributions from both the hydrated dimer and the uppermost bilayer (projection ii). DFT projection is magnified by a factor of eight.

5. Summary

We have applied the combination of MIES, UPS(HeII), FTIR, and TPD spectroscopies successfully to investigate the interaction between acetic acid (AA) and water molecules at acid−water interfaces. We have prepared acid−water interfaces at 80 K, namely, acid layers on thin films of solid water and water adlayers on thin acid films; they were annealed between 80 and 200 K. DFT calculations (see ref 1, preceding paper) were employed successfully for the interpretation of the electron spectra and, moreover, to get information on the electronic structure of the AA−water system by the comparison of the DFT DOS with the electron energy spectra.

Our results are compatible with the DFT results of ref 1, suggesting top-adsorption of AA on ice as cyclic dimers. Above 120 K, changes can be noticed in the MIES, HeII, and IR spectra, indicating a reorganization of the top layer (whereby the cyclic dimers remain stable); our interpretation is that an amorphous-to-supercooled liquid transition (glass transition) takes place in condensed AA around 130 K.

The AA films experience a cyclic dimer-to-poly-crystalline chain transition around 155 K. This transition is attributed to a concerted proton exchange between neighboring AA species. At that stage, some AA and water molecules desorb together. However, the AA chain structure remains stable up to 180 K. As a consequence, H_2O molecules desorb through condensed AA films (around 160 K). As MIES shows, the interaction of H_2O molecules with amorphous AA films, in the initial phase of exposure, does not lead to the formation of a top-adsorbed closed water film at 80 K. Rather, the H_2O molecules become attached to or incorporated into the preexisting AA network by H bonding in a way that the AA molecules remain accessible to the He* probe atoms in MIES; that is, the hydration remains incomplete under these conditions. These H_2O molecules are comparatively weakly bound, and desorb about 20 K earlier than that from ice, indicating that, under these conditions, the interaction of H_2O with AA films is weaker than that with ice films.

Acknowledgment. The cooperation between our institutions was supported by the COST D19 action of the EU.

References and Notes

(1) Allouche, A.; Bahr, S. *J. Phys. Chem. B* **2006**, *110*, 8640.
(2) Casassa, S.; Pisani, C. *J. Chem. Phys.* **2002**, *116*, 9856.
(3) Kondo, M.; Kawanowa, H.; Gotoh, Y.; Souda, R. *J. Chem. Phys.* **2004**, *121*, 8589.
(4) Parent, P.; Laffon, C. *J. Phys. Chem. B* **2005**, *109*, 1547.
(5) Park, S.-C.; Kang, H. *J. Phys. Chem. B* **2005**, *109*, 5124−5132.
(6) Compoint, M.; Toubin, C.; Picaud, S.; Hoang, P.; Girardet, C. *Chem Phys. Lett.* **2002**, *365*, 1.
(7) Picaud, S.; Hoang, P.; Peybernès, N.; Le Calvé, S.; Mirabel, P. *J. Chem. Phys.* **2005**, *122*, 194707.
(8) Kondo, M.; Shibata, T.; Kawanowa, H.; Gotoh, Y.; Souda, R. *Nucl. Instr. Methods Phys. Res., Sect. B* **2005**, *232*, 134−139.
(9) Souda, R. *J. Chem. Phys.* **2003**, *119*, 2774.
(10) Columbia, M. R.; Crabtree, A.; Thiel, P. *Surf. Sci.* **1992**, *271*, 139.
(11) Souda, R. *Chem. Phys. Lett.* **2005**, *413*, 171−175.
(12) Morgner, H. *Adv. Atom. Mol. Opt. Phys.* **2000**, *42*, 387.
(13) Harada, Y.; Masuda, S.; Osaki, H. *Chem. Rev.* **1997**, *97*, 1897.
(14) Bahr, S.; Borodin, A.; Höfft, O.; Kempter, V.; Allouche, A. *J. Chem. Phys.* **2005**, *122*, 234704.
(15) Allouche, A. *J. Chem. Phys.* **2005**, *122*, 234703.
(16) Gao, Q.; Leung, K. T. *J. Phys. Chem. B* **2005**, *109*, 13263.
(17) Gao, Q.; Leung, K. T. *J. Chem. Phys.* **2005**, *123*, 074325.
(18) Krischok, S.; Höfft, O.; Günster, J.; Stultz, J.; Goodman, D. W.; Kempter, V. *Surf. Sci.* **2001**, *495*, 8.
(19) Zondlo, M. A.; Onash, T.; Warshavsky, M. S.; Tolbert, M. A.; Mallich, G.; Arentz, P.; Robinson, M. S. *J. Phys. Chem. B* **1997**, *101*, 10887.
(20) Bally, T. In *Reactive Intermediate Chemistry*; Moss, R., Platz, M., Jones, M., Eds.; Wiley: Hoboken, NJ, 2004; p 797.
(21) Ohno, K.; Takano, S.; Mase, K. *J. Phys. Chem.* **1986**, *90*, 2015.
(22) Carnovale, F.; Gan, T.; Peel, J. *J. Electron. Spectrosc. Relat. Phenom.* **1980**, *20*, 53.
(23) Kimura, K.; Katsumata, S.; Achiba, Y.; Yamazaki, T.; Iwata, S. *Handbook of HeI Photoelectron Spectra of Fundamental Organic Molecules*; Halsted Press: New York, 1990.
(24) Bahr, S. Diploma thesis, TU Clausthal, 2004.
(25) Rovira, C.; Novoa, J. *J. Chem. Phys.* **2000**, *113*, 9208.
(26) Chocholoušvá, J.; Vacek, J.; Hobza, P. *J. Phys. Chem.* **2003**, *2107*, 3086.
(27) Tyrode, E.; Johnson, C. M.; Baldelli, S.; Leygraf, C.; Rutland, M. *J. Phys. Chem. B* **2005**, *109*, 329.
(28) Smith, S. R.; Dohnalek, Z.; Kimmel, G. A. Teeter, G.; Ayotte, P.; Daschbach, J. L.; Kay, B. In *Water in Confining Geometries*; Buch, V., Devlin, J., Eds.; Springer: Berlin, 2003.
(29) Borget, F.; Chiavassa, T.; Aycard, J. *Chem. Phys. Lett.* **2001**, *348*, 425.
(30) Borget, F.; Chiavassa, T.; Allouche, A.; Aycard, J. *J. Phys. Chem. B* **2001**, *105*, 449.
(31) Borget, F.; Chiavassa, T.; Allouche, A.; Marinelli, F.; Aycard, J. *J. Am. Chem. Soc.* **2001**, *123*, 10668.
(32) Jenniskens, P.; Blake, D. *Science* **1994**, *265*, 753.
(33) Xu, C.; Koel, B. E. *J. Chem. Phys.* **1995**, *102*.
(34) Haurie, M.; Novak, A. *J. Chim. Phys.* **1965**, *62*, 147.
(35) Krause, P. F.; Katon, J. E.; Rogers, J. M.; Phillips, D. B. *Appl. Spectrosc.* **1977**, *31*, 110.
(36) Haurie, M.; Novak, A. *Spectrochim. Acta* **1965**, *21*, 1217−1228.
(37) Millikan, R.; Pitzer, K. *J. Am. Chem. Soc.* **1958**, *80*, 3515.
(38) Raval, R.; Munro, S. *J. Electron. Spectrosc. Relat. Phenom.* **1993**, *64/65*, 461.
(39) Ohtani, T.; Kubota, J.; Wada, A.; Kondo, J.; Domen, K.; Hirose, C. *Surf. Sci.* **1996**, *368*, 270.
(40) Cyriac, J.; Pradeed, T. *Chem. Phys. Lett.* **2005**, *402*, 116.
(41) Souda, R. *J. Chem. Phys.* **2005**, *122*, 134711.